# DNA topology dictates strength and flocculation in DNA-microtubule composites

Karthik R. Peddireddy[1], Davide Michieletto[2,3], Gina Aguirre[1], Jonathan Garamella[1], Pawan Khanal[1], and Rae M. Robertson-Anderson[1,*]

[1]*Department of Physics and Biophysics, University of San Diego, 5998 Alcala Park, San Diego, CA 92110, United States*

[2]*School of Physics and Astronomy, University of Edinburgh, Peter Guthrie Tait Road, Edinburgh, EH9 3FD, UK,* [3]*MRC Human Genetics Unit, Institute of Genetics and Molecular Medicine University of Edinburgh, Edinburgh EH4 2XU, UK*

## SUPPLEMENTARY INFORMATION



### Section 1. Experimental Section

*DNA:*Double-stranded 115 kilobasepair DNA is prepared by replication of cloned bacterial artificial chromosomes (BACs) in *E. Coli*, followed by extraction, purification, and concentration using custom-designed protocols described elsewhere[1,2]. Supercoiled BAC DNA constructs are enzymatically treated with MluI or topoisomerase I (New England Biolabs) to convert the supercoiled constructs to linear (L) or ring (R) topology, respectively. Both linear and ring DNA stock solutions are suspended in TE10 buffer (10 mM Tris-HCl (pH 8), 1 mM EDTA, 10 mM NaCl) at concentrations ($c$) of 1.9 mg/ml and 1.1 mg/ml, respectively. DNA concentration for experiments is fixed at $c$=0.65 mg/ml, which corresponds to $2.5c_e$ where $c_e$ is the critical entanglement concentration[3]. This concentration translates to $N_e \approx 5$ entanglements for linear DNA, computed using traditional Doi-Edwards theory, which predicts $N_e = (4/5)cRT/(MG^0)$, where $M$ is the molecular weight of the polymer and $G^0$ is the plateau modulus[4]. $G^0$ is obtained from linear microrheology experiments (Figure S1).

*Microtubules (MT):* Porcine brain dark tubulin (T240) and rhodamine-labeled tubulin (TL590M) are obtained from Cytoskeleton. Tubulin stock solutions (45.5 μM) containing 9:1 dark:labeled tubulin in PEM100 buffer (100 mM PIPES (pH 6.8), 2 mM $MgCl_2$, 2mM EGTA) are flash-frozen in liquid nitrogen and stored at -80°C. To form DNA-microtubule composites, microtubules are grown directly in DNA solutions by adding 2 mM GTP, to enable polymerization, and 10 μM Taxol to stabilize polymerized microtubules.

*Sample preparation:* DNA and tubulin are mixed slowly and thoroughly using wide-bore pipette tips, to prevent shearing of DNA, then introduced into sample chambers through capillary action. Sample chambers

(2 cm x 0.3 cm x 0.01 cm) are made with a microscope glass slide and coverslip separated by two layers of double-sided tape and hermetically sealed with epoxy. To polymerize tubulin dimers and form DNA-microtubule samples, sample chambers are incubated at 37°C for two hours, resulting in repeatable and reliable polymerization of microtubules in the DNA solutions. As an alternative method to forming composites, we also polymerized microtubules prior to adding to DNA solutions and loading into the sample chamber. However, this method resulted in random flow alignment of microtubules that occurred when introducing the DNA-MT mixtures into the sample chambers, so the data is not shown here.

*Microrheology:* For microrheology experiments, a trace amount of polystyrene beads (Polysciences, Inc.) of radius $R$=2.25 μm are added to the DNA-tubulin mixtures prior to microtubule polymerization. Beads are coated with Alexa-488 BSA to prevent DNA adsorption and for fluorescence visualization. 0.1 wt% Tween 20 is added to reduce DNA and bead adsorption to the sample chamber walls. An oxygen scavenging system (45 μg/mL glucose, 43 μg/mL glucose oxidase, 7 μg/mL catalase, and 5 μg/mL β-mercaptoethanol) is added to inhibit photobleaching.

We use optical tweezers microrheology to determine linear and nonlinear rheological properties of the DNA-MT composites (Figure 1). Details of the experimental procedures and data analysis, briefly summarized below, have been described in detail in refs [5,6]. The optical trap, built around an Olympus IX71 epifluorescence microscope, is formed from a 1064 nm Nd:YAG fiber laser (Manlight) focused with a 60x 1.4 NA objective (Olympus). Forces exerted by the DNA-MT composites on the trapped beads are determined by recording the laser beam deflections via a position sensing detector (Pacific Silicon Sensors) at 20 kHz. The trap is calibrated for force measurement using the stokes drag method.

Linear viscoelastic properties are determined from thermal fluctuations of a trapped microsphere, measured by recording the associated laser deflections for 180 seconds at 20 kHz. Linear viscoelastic moduli, i.e. the elastic modulus $G'(\omega)$ and the viscous modulus $G''(\omega)$, were extracted from the thermal fluctuations using the generalized Stokes-Einstein relation (GSER) as described in ref [7]. The procedure requires extracting the normalized mean-squared displacements ($\pi(\tau) =< r^2(\tau) >/2 < r^2 >$) of the thermal forces, averaged over all trials, which is then converted into the Fourier domain via:

$$-\omega^2\,\pi(\omega) = \left(1 - e^{-i\omega\tau_1}\right)\frac{\pi(\tau_1)}{\tau_1} + \dot{\pi}_\infty e^{-i\omega t_N} + \sum_{k=2}^{N}\left(\frac{\pi_k - \pi_{k-1}}{\tau_k - \tau_{k-1}}\right)\left(e^{-i\omega\tau_{k-1}} - e^{-i\omega\tau_k}\right),$$

where $\tau$, 1 and N represent the lag time and the first and last point of the oversampled $\pi(\tau)$. $\dot{\pi}_\infty$ is the extrapolated slope of $\pi(\tau)$ at infinity. Oversampling is done using the MATLAB function PCHIP. $\pi(\omega)$ is related to viscoelastic moduli via:

$$G^*(\omega) = G'(\omega) + iG''(\omega) = \left(\frac{k}{6\pi R}\right)\left(\frac{1}{i\omega\pi(\omega)} - 1\right),$$

where $R$ and $k$ represent the radius of the microsphere and trap stiffness. We computed the complex viscosity $\eta^*(\omega)$ via $\eta^*(\omega) = [(G'(\omega))^2+(G''(\omega))^2]^{1/2}/\omega$.

Nonlinear microrheology measurements are performed by displacing a trapped microsphere, $x = 30\ \mu m$, through the sample at speeds of $v$ = 2.5 – 120 μm/s using a piezoelectric nanopositioning stage (Mad City Laboratories) to move the sample relative to the microsphere. We convert the distance to strain via $\gamma = x/2R$, and convert speeds to strain rates via $\dot{\gamma}=3v/\sqrt{2}R$ (2.4-113 $s^{-1}$) [8]. The strain of 6.7 is much higher than the critical value of 1 for nonlinearity and our chosen strain rates are higher than the terminal relaxation frequencies $\omega_T = \lim_{\omega\to 0} \omega G''/G'$ of all DNA-MT composites under investigation. For both linear and nonlinear measurements, all data is recorded at 20 kHz, and at least 15 trials are conducted, each with a new microsphere in an unperturbed location. Presented data is an average of all trials.

*Confocal microscopy:* Microtubules in DNA-MT composite networks are imaged using a Nikon A1R laser scanning confocal microscope with a 60× 1.4 NA objective. 10% of tubulin dimers comprising microtubules are rhodamine-labeled to enable imaging using a 561 nm laser with 561 nm excitation and 595 nm emission filters. DNA in composites is unlabeled. 512×512 pixel images (212 μm ×212 μm) are taken at 20 different locations in the sample for each DNA-MT composite. Spatial image autocorrelation analysis is performed on each image using a custom-written python script[9,10]. Autocorrelation curves, $g(r)$, for each image are obtained by measuring the correlation in intensity $I(r)$ as a function of distance $r$.[9] Specifically, $g(r)$ is computed from $I(r)$ via:

$$g(r) = \frac{F^{-1}(|F(I(r))|^2)}{[I(r)]^2}$$

where $F$ and $F^{-1}$ represent fast Fourier and inverse Fourier transforms. The correlation length ξ is obtained by fitting autocorrelation curves to $g(r) = Ae^{r/\xi}$.

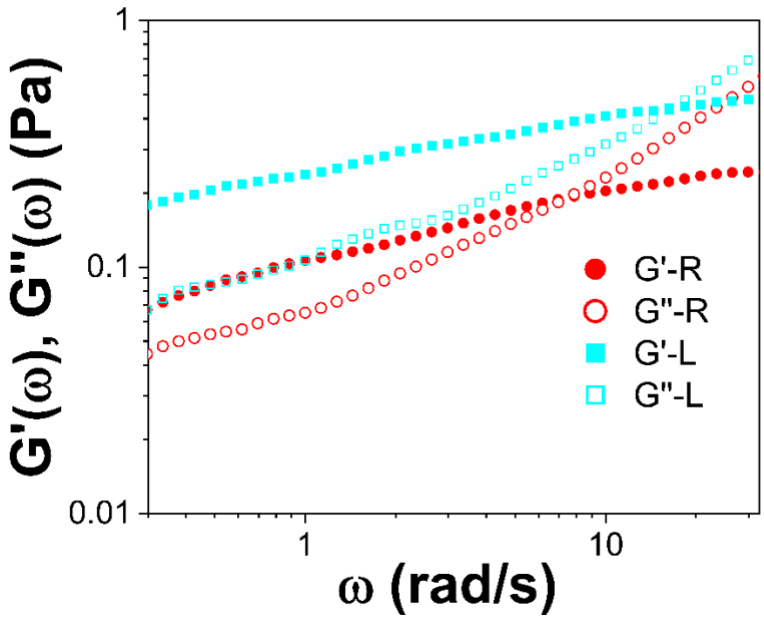


**Figure S1. Linear frequency-dependent viscoelastic moduli for 0.65 mg/ml solutions of 115 kbp linear (squares) and ring (circles) DNA.** Elastic (*G'(ω)*, closed symbols) and viscous moduli (*G"(ω),*open symbols) versus angular frequency *ω*.

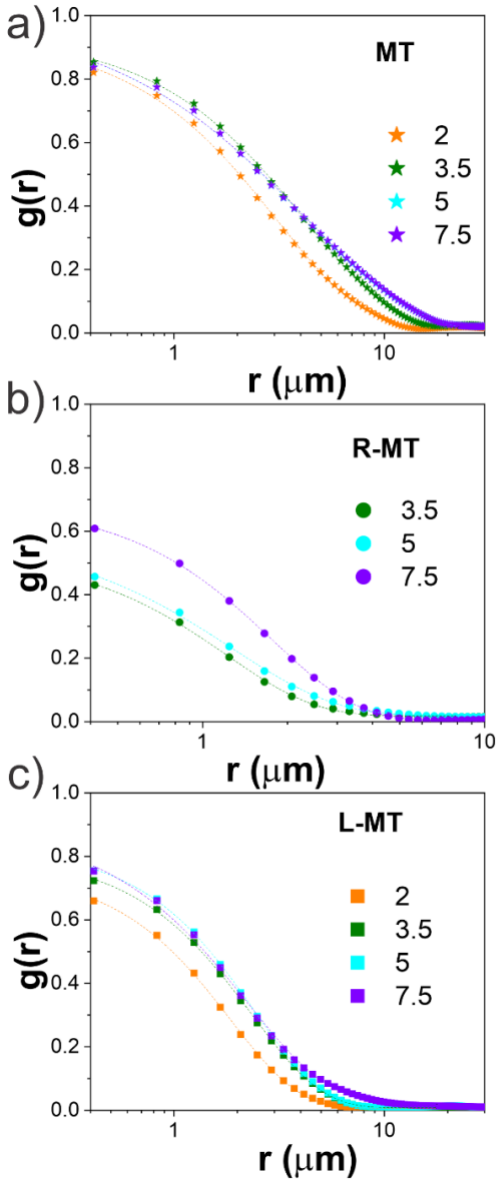


**Figure S2. Average spatial image autocorrelation curves of DNA-MT composites**. Each curve is an average of $g(r)$ curves computed for 20 different images of rhodamine-labeled microtubules taken at different locations of 2 independent samples for (a) microtubules without DNA, (b) R-MT composites and (c) L-MT composites with varying tubulin concentrations shown in □M in the legends.

**Section 2: Theory for phase behavior of a composite of stiff and flexible polymers**

The free energy of a solution of hard rod-like colloids and flexible polymers is

$$F = F_R(N_R, V, [f]) - \Pi(\mu_P)V_f$$

Where $F_R$ is the Helmoltz free energy of a system of $N_R$ rods in a volume $V$ and $\Pi = \mu_p n_p$ is the osmotic pressure exerted by a reservoir of polymer molecules, equal to the chemical potential multiplied by the number density of polymer molecules. Finally, $V_f$ is the free volume available to the polymer computed by the average volume available to polymers and $f$ the orientation distribution of the rods. This function captures the fact that the rods can be in an isotropic or nematic state and assumes a shape that minimizes the free energy.

*Free energy of rod colloids*

To express $F_R$ as a function of the density including corrections beyond the second virial coefficient we use the Scaled Particle Theory (SPT) description[11,12]:

$$\frac{F_R}{N_c k_B T} = \log n_c - \log(1-\phi) + \sigma + X_2 \frac{\phi}{1-\phi} + \frac{1}{2} X_3 \left(\frac{\phi}{1-\phi}\right)^2 \quad (1)$$

Where $n_c = N_c/V$ is the colloid particle density,

$$\phi = n_c \left(\frac{\pi}{6} D^3 + \frac{\pi}{4} D^2 L\right) \quad (2)$$

their volume fraction. The coefficients $X_2$ and $X_3$ are given by

$$X_2 = 3 + \frac{3(\gamma-1)^2}{3\gamma - 1}\rho[f]$$

$$X_3 = \frac{12\gamma(2\gamma-1)}{(3\gamma-1)^2} + \frac{12\gamma(\gamma-1)^2}{(3\gamma-1)^2}\rho[f]$$

Where $\gamma = (L+D)/D$ and the quantities

$$\sigma = \int d\Omega\, f \log(4\pi f)$$

$$\rho = \frac{4}{\pi}\int\int d\Omega\, d\Omega'\, f f' \sin(\theta)$$

And $\theta$ is the angle between two rod-like colloids. To simplify the calculations, we will use the ansatz that $f$ is a Gaussian distribution – this reduces the problem of finding the free energy minimizing orientation distribution of colloids to that of minimizing a variational parameter $\alpha$ defined via the function $f(\theta) = \frac{\alpha}{4\pi} e^{-\frac{1}{2}\alpha\theta^2}$ for $0 < \theta < \frac{\pi}{2}$ and $f(\theta) = \frac{\alpha}{4\pi} e^{-\frac{1}{2}\alpha(\pi-\theta)^2}$ for $\frac{\pi}{2} < \theta < \pi$. Importantly, using large $\alpha$ (nematic phase), one finds

$$\sigma = \sigma(\alpha) \simeq \log(\alpha) - 1 \tag{3}$$

and

$$\rho = \rho(\alpha) \simeq 4/\sqrt{\pi\alpha}\,. \tag{4}$$

In the isotropic phase, these terms are $\sigma = 0$ and $\rho = 1$.

*Free volume of polymers*

To obtain the free volume available to polymers, we employ Widom's particle insertion method, which relates the chemical potential of a polymer species to work needed to insert one such a polymer in the system. We thus write

$$\mu_p = k_B T \log\frac{N_p}{V_f} = k_B T\,(\log\frac{N_p}{V} - \log\frac{V_f}{V})$$

Which also equals

$$\mu_p = k_B T \log\frac{N_p}{V} + W$$

Putting the two equations together one obtains

$$\nu = \frac{V_f}{V} = e^{-W/k_B T} = (1-\phi)\exp(-Ay - By^2 - Cy^3) \tag{5}$$

Where $y = \phi/(1-\phi)$ and

$$A = \frac{6\gamma}{3\gamma-1}q + \frac{3(\gamma+1)}{3\gamma-1}q^2 + \frac{2}{3\gamma-1}q^3$$

$$B = \frac{1}{2}\left(\frac{6\gamma}{3\gamma-1}\right)^2 q^2 + \left(\frac{6}{3\gamma-1} + \frac{6(\gamma-1)^2}{3\gamma-1}\rho[f]\right)q^3$$

$$C = \frac{2}{3\gamma-1}\left(\frac{12\gamma(2\gamma-1)}{(3\gamma-1)^2} + \frac{12\gamma(\gamma-1)^2}{(3\gamma-1)^2}\rho[f]\right)q^3$$

With $q = \sigma/D$is the ratio between the diameter of the flexible polymer and the diameter of the rod-like colloid and $\gamma = (L+D)/D$[11].

Combining Eqs. (3-5) into (1) yields a semi-grand canonical free energy with one ($\alpha$) variational parameter that needs to be tuned to its free-energy-minimising value. To find it, we numerically compute the minimum of Eq. (1) as a function of $\alpha$ and for different values of $n_c$ (or equivalently $\phi$) and we store its root $\alpha_m(\phi)$.

This parameter is found to undergo a jump from 0 to >0 at a critical value $\phi_c$ that signals the onset of the nematic transition. To find the binodals we then solve the standard coexistence equations, i.e.

$$\mu_c(\phi_I, f_I) = \mu_c(\phi_N, f_N)$$

$$\Pi_c(\phi_I, f_I) = \Pi_c(\phi_N, f_N)$$

Where $\mu_c = \frac{dF^*}{dN_c} = \frac{d(F_R^*/V)}{dn_c} - \Pi_p \frac{dv}{dn_c}$ is the total chemical potential (evaluated from $F^* = F(\phi, \alpha = \alpha_m)$ ) and $\Pi_c = -\frac{dF^*}{dV} = \Pi_0 + \Pi_p(v - n_c \frac{dv}{dn_c})$ is the pressure (to compute these we make use of $\frac{N_c}{V} = n_c = \phi / \left( \frac{\pi}{6} D^3 + \frac{\pi}{4} D^2 L \right)$). The coexistence equations essentially encode the fact that, in equilibrium, both chemical potential and pressure must be equal in the two (isotropic and nematic) phases.

**References**


1 Robertson, R. M., Laib, S. & Smith, D. E. Diffusion of isolated DNA molecules: Dependence on length and topology. *Proceedings of the National Academy of Sciences* **103**, 7310-7314 (2006).

2 Laib, S., Robertson, R. M. & Smith, D. E. Preparation and Characterization of a Set of Linear DNA Molecules for Polymer Physics and Rheology Studies. *Macromolecules* **39**, 4115-4119 (2006).

3 Robertson, R. M. & Smith, D. E. Self-Diffusion of Entangled Linear and Circular DNA Molecules: Dependence on Length and Concentration. *Macromolecules* **40**, 3373-3377 (2007).

4 Doi, M. & Edwards, S. F. *The Theory of Polymer Dynamics* Vol. **73** (Oxford University Press, 1986).

5 Falzone, T. T., Blair, S. & Robertson-Anderson, R. M. Entangled F-actin displays a unique crossover to microscale nonlinearity dominated by entanglement segment dynamics. *Soft Matter* **11**, 4418-4423 (2015).

6 Gurmessa, B. *et al.* Counterion crossbridges enable robust multiscale elasticity in actin networks. *Physical Review Research* **1**, 013016 (2019).

7 Tassieri, M., Evans, R. M. L., Warren, R. L., Bailey, N. J. & Cooper, J. M. Microrheology with optical tweezers: data analysis. *New Journal of Physics* **14**, 115032 (2012).

8 Squires, T. M. Nonlinear Microrheology: Bulk Stresses versus Direct Interactions. *Langmuir* **24**, 1147-1159 (2008).

9 Robertson, C. & George, S. C. Theory and practical recommendations for autocorrelation-based image correlation spectroscopy. *Journal of biomedical optics* **17**, 080801 (2012).

10 Lee, G. *et al.* Active Cytoskeletal Composites Display Emergent Tunable Contractility and Restructuring. *arXiv preprint arXiv:2104.04113* (2021).

11 Lekkerkerker, H. N. W. & Stroobants, A. Phase behaviour of rod-like colloid+flexible polymer mixtures. *Il Nuovo Cimento D* **16**, 949 (1994).

12 Warren, P. B. Depletion effect in a model lyotropic liquid crystal-theory. *Journal de Physique I* **4**, 237-244 (1994).